10 November 2000

ELSEVIER

Chemical Physics Letters 330 (2000) 231–236

CHEMICAL PHYSICS LETTERS

www.elsevier.nl/locate/cplett

Evaluation of the energetics of electron trap states at the nanocrystalline titanium dioxide/aqueous solution interface via time-resolved photoacoustic spectroscopy

Svetlana Leytner, Joseph T. Hupp *

Department of Chemistry and Institute for Environmental Catalysis, Northwestern University, 2145 Sheridan Road, Evanston, IL 60208-3113, USA

Received 24 July 2000; in final form 15 September 2000

Abstract

Time-resolved photoacoustic spectroscopy (TRPAS) has been employed to probe directly the trap state energetics of photogenerated electrons in nanocrystalline colloidal titanium dioxide dispersed in aqueous solution. Deconvolution of the photoacoustic signals obtained following bandgap excitation allowed for separation of components associated with conduction band electron trapping, trapped electron–hole recombination, and a slower recombination step. The results indicate that the lifetime of the electron–hole pair is on the order of 25 ns with about 60% of the trapped electrons recombining on this time scale. The electron trapping sites were determined to lie, on average, 0.8 eV below the conduction band edge.

1. Introduction

Nanocrystalline titanium dioxide semiconductor systems with large effective surface areas, and consequently, high densities of surface states have been the subject of extensive investigation because of their promise in photovoltaic [1–5], photocatalytic [6,7], and battery applications [8]. The efficiencies of these materials in photovoltaic and photocatalytic applications depend strongly upon the trapping and recombination energetics and dynamics of photogenerated charge carriers, i.e., electrons and holes. We reasoned that if the pertinent trap state lifetimes exceeded ca. 10 ns, time-resolved photoacoustic spectroscopy (TRPAS) might offer a particularly direct way of evaluating their energetics. Briefly, TRPAS involves the rapid deposition of energy into a system, generally via pulsed laser excitation, and the subsequent release of energy as heat that is detected as a pressure wave by a piezoelectric transducer [9–11]. If the heat release involves system relaxation through a well-defined and thermally equilibrated intermediate state, and if the heat-release dynamics can be appropriately deconvoluted, the enthalpy content of the intermediate state, with respect to the ground state, can be quantitatively evaluated.

For colloidal TiO_2, electron traps can be rapidly populated by several means including dye injection, pulse radiolysis, and bandgap excitation. Here we have focused on the bandgap approach: the absorption of a UV photon creates an electron–hole pair by promoting an electron from the valence band to the conduction band; the

* Corresponding author. Fax: +1-847-491-7713.
E-mail address: jthupp@chem.nwu.edu (J.T. Hupp).

0009-2614/00/$ - see front matter
PII: S0009-2614(00)01112-X

electron is then rapidly (<500 fs) [12,13] trapped at a Ti^{4+} surface site [14] (see Scheme 1). Hole trapping takes place at surface OH^- sites [15–17] and is known to occur on a much longer time scale, presumably due to the larger effective mass of the hole versus the electron [12,18]. It should be noted, however, that Serpone et al. [19] have reported that the transient spectrum of the trapped hole is fully developed within 30 ps. It is generally accepted that at high electron–hole pair concentrations the trapped electron recombines with a free or trapped hole following second-order kinetics, although the recombination rate constants reported from different labs for differing TiO_2 preparations disagree [12,18,20–22]. Additional studies indicate that recombination reaction has two components: a fast picosecond process and a slower process occurring at times greater than 20 ns. The idea of dynamically distinct shallow and deep-trapped states has been advanced to account for the results [13,23]. For 12 nm diameter TiO_2 particles, under conditions of low charge carrier occupancy, Rothenberger et al. [18] report that the electron–hole recombination process is first order with an electron–hole pair lifetime of 30 ± 15 ns – a time scale compatible with TRPAS based on piezoelectric detection of pressure waves in the time domain. Recently, Stopper and Dohrmann [24] published the results of time-resolved photoacoustic measurements on 2.4 nm colloidal TiO_2 particles in aqueous solution. Deconvolution of the sample signal unveiled that about 88% of the absorbed energy were released promptly (within the time response of the instrument) while

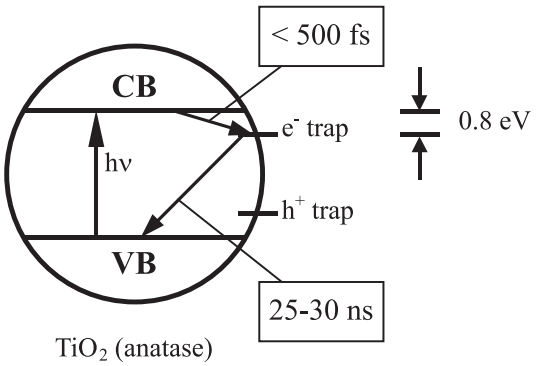

Scheme 1.

12% were stored for at least 2 μs. The latter was attributed to the fast formation of long-lived $OH^{\cdot}_{(aq)}$ and $OH^{\cdot}_{2\ (aq)}$ radicals in oxygenated aqueous solution of nanocrystalline TiO_2. We focus here, however, on processes occurring on a shorter time scale in oxygen-free solutions – our interests being trap state energetics, rather than radical product formation.

We describe below the application of TRPAS to the problem of electron trap state energies at the colloidal TiO_2/aqueous solution interface. It should be noted that the energetics of electron trap states of various TiO_2 *electrode*/solution interfaces have been evaluated by a variety of experimental methodologies. For example, for *n*-type single-crystal rutile electrodes, trap sites have been shown by impedance measurements to lie 0.8 eV below the conduction band edge [25]. For the (0 0 1) surface of a highly doped *n*-type TiO_2 crystal, a trap depth of 0.3 eV has been derived using scanning tunneling microscopy [26]. For a nanocrystalline TiO_2 electrode consisting of sintered anatase particles with an average diameter of 15 nm, the dependence of the charge accumulation rate constant on the initially applied potential has been used to infer the existence of an intraband state about 0.7 eV below the conduction band edge [27]. Subsequent spectroelectrochemical investigations of nanocrystalline TiO_2 electrodes prepared from Degussa P25 particles indicated the presence of traps at ca. 0.5–0.6 eV below the conduction band edge [28]. Similar studies of electrode films composed of small anatase particles showed that traps are present at about 0.5 eV below the conduction band edge [29]. While these findings offer very useful points of reference, none of the corresponding methodologies is applicable to colloidal semiconductor/solution interfaces. We find that the photoacoustic technique can provide kinetic and thermodynamic information on the transients associated with the population and depopulation of electron traps.

2. Experimental

Colloidal titanium dioxide (average particle size ca. 5 nm) was prepared via the acidic hydrolysis of

titanium isopropoxide (Aldrich) using published methods [30]. The initially prepared solution was then diluted with acidified water (pH = 2) to achieve a particle concentration of ca. 3 μM. Samples were purged with solvent-saturated argon prior to the experiments. All experiments were run with unprotected sols at pH = 2. The absorbances of a reference compound, Na_2CrO_4 (98%, Aldrich), and a sample were adjusted to identical values (±3%) – generally about 0.3 at 355 nm. The minor contribution of light scattering to the extinction spectrum of the nanocrystalline colloidal TiO_2 solution was taken into account.

In the photoacoustic setup, sample excitation was achieved by using the third harmonic of a Q-switched mode-locked Nd:YAG laser (355 nm, 10 Hz) featuring a pulse width of 250 ps [31]. The excitation beam was collimated and then passed through a rectangular slit (0.3 × 5 mm). This permitted transient lifetimes as brief as ca. 20 ns and as long as roughly 1000 ns to be resolved. Part of the beam was directed into a photodiode used as an energy reference. Signal detection was accomplished using a 10 MHz piezoelectric transducer (V111-RM, Panametrics) that was affixed to the wall of a 1 cm quartz cuvette. Signals were amplified with a preamplifier (Panametrics, model 5670) interfaced to a LeCroy 9450 350 MHz oscilloscope connected to a PC. All experiments were carried out with laser fluences that were sufficiently low (ca. 15 μJ/pulse) to yield a zero-intercept linear variation of the photoacoustic signal amplitude with pulse energy. The signal amplitude was operationally defined as the difference between the first maximum and the first minimum of the experimental waveform. Sound Analysis version 1.31A software (Quantum Northwest, Spokane, Washington) was utilized for data analysis.

3. Results and discussion

Fig. 1 shows an example of the photoacoustic waveform obtained upon bandgap excitation of the nanocrystalline TiO_2/aqueous solution sample at 24°C. The signal generated by the sodium chromate reference solution is shown for comparison. A best-fit simulation curve and the corresponding residuals are also shown. From the simulation via a standard deconvolution procedure [32] were extracted the lifetime, τ_i, and signal amplitude, φ_i, corresponding to each of ith decay processes following photon absorption. In this analysis, the sample waveform was treated as a convolution of the rapidly relaxing reference signal (used as an instrument response function) and a multiexponential decay that describes evolution of the sample signal in time. In order for the reference signal to be employed quantitatively, it is important that the reference compound release all of its excitation energy promptly in the form of heat [10]. For the analysis here, the deconvolution of the experimental sample waveforms yielded a two-component fit with τ_1 always being less than 1 ns and τ_2 being on the order of 25–30 ns. In addition, signal deconvolution revealed that not all of the excitation energy was released within the time window accessible by deconvolution analysis; some of it was stored in a longer-lived species. This third component decayed sufficiently slowly ($\tau \gg$ 1000 ns) to be ignored in the deconvolution.

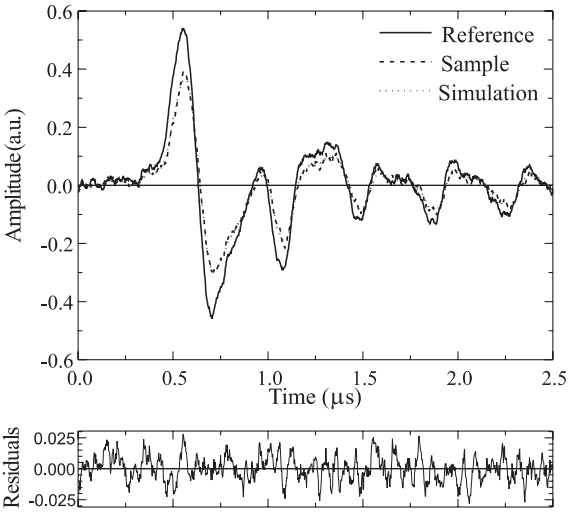

Fig. 1. Photoacoustic signals for the reference Na_2CrO_4 (solid line) and nanocrystalline colloidal TiO_2 sample (dashed line) in aqueous solution at 24°C, together with a simulation curve (dotted line).

The fastest process revealed by deconvolution analysis is attributed to conduction band electron trapping, in agreement with the generally accepted

concept of the prompt (hundreds of femtoseconds) electron trapping process. Fixing this parameter at any value between 1 fs and 1 ns produced similar amplitude values. Consistent with the report by Rothenberger et al. [18] we assign the second component to recombination of the trapped electron and delocalized hole. The origin of the third component is less clear, although its existence has been documented previously [12,18]. One explanation is that scavenging of either the electron or the hole occurs – for example, by adventitious impurities such as traces of dissolved oxygen or by the solvent itself – leaving the remaining charge orphaned on the particle until a second scavenging event occurs. Under different conditions (air-saturated solutions), Stopper and Dohrmann [24] have noted in their photoacoustic work that photogenerated holes may oxidize water and trapped electrons may reduce dissolved oxygen to yield, respectively, $OH^{\cdot}_{(aq)}$ and $OH^{\cdot}_{2\ (aq)}$. In any case, we will focus the remainder of the analysis and discussion on the process associated with τ_2.

From a knowledge of the laser energy, laser beam geometry, and sample concentration we estimate that on average about 0.8 photons are absorbed per particle. Assuming that every absorbed photon generates one electron–hole pair, 0.8 pairs are created per colloidal particle. This value is sufficiently small to satisfy the condition for simple first-order charge recombination kinetics previously described by Rothenberger et al. [18]. Increasing the laser fluence in photoacoustic experiments resulted in an inability to describe the decay data satisfactorily with a two-component fit. This was expected since sufficiently high laser fluences will produce a large enough number of charge carriers per particle to induce second-order kinetics and an acceleration of the recombination process [18]. This in turn yields recombination rates that exceed the time resolution of the photoacoustic setup.

TRPAS experiments involve measuring the time-evolving pressure wave produced by the expansion or contraction of the medium as a result of heat release via nonradiative excited state relaxation. In addition to the thermal changes, sample pressure waves also contain contributions from changes in reaction volume induced by the chemical or structural changes in the system. The separation of these two components can be accomplished by recognizing that the magnitude of the thermal part of the signal, unlike the reaction volume change component, depends on the thermoelastic properties of the medium – specifically, the ratio $C_p\rho/\beta$, where C_p is the heat capacity, ρ the mass density, and β is the thermal expansion coefficient of the solvent. In the experiments described here, advantage was taken of the strong temperature dependence of the thermal expansion coefficient for water, and the desired terms were separated on the basis of acoustic transient measurements over the temperature range of 10–24°C.

To obtain the total enthalpy change, ΔH_i, and the reaction volume change, ΔV_i, corresponding to the ith excited state decay, the following equation was employed [10]:

$$\mathrm{E}_\lambda \varphi_i = \Phi_{\mathrm{R},i}\Delta H_{\mathrm{R},i} + \Phi_{\mathrm{R},i}\Delta V_{\mathrm{R},i}\left(\frac{C_p\rho}{\beta}\right) = \Delta H_i + \Delta V_i\left(\frac{C_p\rho}{\beta}\right). \quad (1)$$

In the equation, E_λ is the excitation energy (337 kJ/mole at 355 nm), and $\Phi_{\mathrm{R},i}$, $\Delta H_{\mathrm{R},i}$, and $\Delta V_{\mathrm{R},i}$ are the quantum yield, the enthalpy and the volume change for the ith step. Fig. 2 shows the deconvoluted photoacoustic amplitudes as a function of the thermoelastic properties of the solvent plotted according to Eq. (1). The values obtained from the linear fit intercepts and slopes are: $\Delta H_1 = 90$ kJ/mole; $\Delta H_2 = 154$ kJ/mole; $\Delta V_1 = 2.9$ ml/mole; $\Delta V_2 = -1.7$ ml/mole. The $\Delta H_1 = 90$ kJ/mole value represents the amount of heat released upon trapping of the photogenerated electrons occurring on the femtosecond time scale. Given this information, the total enthalpy content of the trapped states, i.e., both the short (25–30 ns) and much longer-lived components, can be calculated as follows:

$$\Delta H_{tr} = \frac{E_\lambda - \Delta H_1}{\varphi_{tr}}, \quad (2)$$

where φ_{tr} is the electron trapping efficiency. Assuming φ_{tr} is close to unity, $\Delta H_{tr} = 247$ kJ/mole or 2.5 eV relative to the valence band edge. Ignoring entropic effects, this analysis indicates that electron

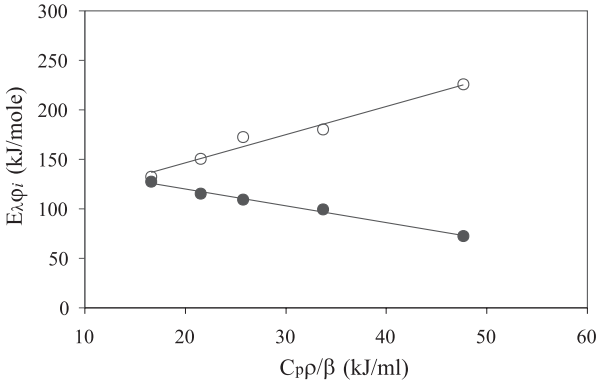

Fig. 2. Deconvoluted photoacoustic amplitudes $E_\lambda\varphi_1$ (open circles) and $E_\lambda\varphi_2$ (filled circles) as a function of thermoelastic parameters of the solvent $(C_p\rho/\beta)$ (see Eq. (1)). The experimental temperatures from left to right are 24°C, 19°C, 16°C, 13°C, and 10°C.

trap sites lie, on average, about 0.8 eV below the conduction band edge; this finding is consistent with the electron trapping energy values obtained earlier for the single-crystal rutile electrodes and nanocrystalline TiO_2 films [25,27]. Using a value of $\Delta H_2 = 154$ kJ/mole, which represents the heat release corresponding to the faster electron–hole recombination process, and assuming that all trap sites have similar energies, we can estimate that approximately 60% of the electrons recombine on the 30 ns time scale, while 40% of the electrons live longer than about 1 μs (the long-time resolution limit of the experiment as currently configured).

Photoacoustic experiments also report on volume changes (see Eq. (1)). ΔV_1 is associated with the initial fast vibrational cooling/phonon relaxation, charge separation, and electron trapping steps, while ΔV_2 describes the recombination process. The reaction volume change is related to the entropy change associated with a particular photoinduced reaction process [33,34]. Although quantitative conclusions on the entropy changes cannot be drawn based on the ΔV values obtained, qualitatively we can say that they have the same sign. If the reaction volume changes are attributed primarily to solvent electrostriction phenomena, the combined cooling, charge separation, and electron trapping steps are accompanied by a net expansion of the solvent around the TiO_2 particle and an entropy increase, while the charge recombination step induces solvent contraction and an entropy decrease.

Finally, we have recently found that the TRPAS technique is also applicable to dye-sensitized reactions at metal-oxide semiconductor/solution interfaces. We hope to report shortly on these studies.

4. Conclusions

The TRPAS has been applied to the electron transfer reaction at the solid/liquid interface to evaluate directly the trap state energetics of photogenerated electrons in nanocrystalline colloidal titanium dioxide dispersed in aqueous solution. The electron trapping sites have been shown to be present at about 0.8 eV below the conduction band edge. Deconvolution of photoacoustic signals indicated that approximately 60% of trapped electron–hole pairs recombine on the time scale of about 25 ns, while 40% of the electrons live longer than about 1 μs.

Acknowledgements

We gratefully acknowledge Professor Kenneth Spears for loan of laser equipment. We thank the Office of Naval Research and the Institute for Environmental Catalysis at Northwestern University for financial support.

References

[1] A. Hagfeld, M. Gratzel, Chem. Rev. 95 (1995) 49.
[2] G.J. Meyer, P.C. Searson, Interface 2 (1993) 23.
[3] N.S. Lewis, J. Phys. Chem. 102 (1998) 4843.
[4] S.G. Yan, L.A. Lyon, B.I. Lemon, J.S. Preiskorn, J.T. Hupp, J. Chem. Educ. 74 (1997) 657.
[5] B.A. Gregg, A. Zaban, S. Ferrere, Z. Phys. Chem. 212 (1999) 11.
[6] M.R. Hoffman, S.T. Martin, W. Choi, D.W. Bahnemann, Chem. Rev. 95 (1995) 69.
[7] D.C. Schemelling, K.A. Gray, P.V. Kamat, Environ. Sci. Technol. 30 (1996) 2547.
[8] S.Y. Huang, L. Kavan, I. Exnar, M. Gratzel, J. Electrochem. Soc. 142 (1995) L142.
[9] J.E. Rudzki, J.L. Goodman, K.S. Peters, J. Am. Chem. Soc. 107 (1985) 7849.
[10] S.E. Braslavsky, G.E. Heibel, Chem. Rev. 92 (1992) 1382.
[11] K.A. Walters, K.S. Schanze, Spectrum 11 (1998) 2.
[12] D.P. Colombo Jr., K.A. Roussel, J. Saeh, D.E. Skinner, J.J. Cavaleri, R.M. Bowman, Chem. Phys. Lett. 232 (1995) 207.
[13] D.E. Skinner, D.P. Colombo Jr., J.J. Cavaleri, R.M. Bowman, J. Phys. Chem. 99 (1995) 7853.
[14] R.F. Howe, M. Gratzel, J. Phys. Chem. 89 (1985) 4495.
[15] D. Bahnemann, A. Henglein, J. Lilie, L. Spanhel, J. Phys. Chem. 88 (1984) 709.
[16] D. Bahnemann, A. Henglein, L. Spanhel, Faraday Discuss. Chem. Soc. 78 (1984) 151.
[17] D. Lawless, N. Serpone, D. Meisel, J. Phys. Chem. 95 (1991) 5166.
[18] G. Rothenberger, J. Moser, M. Gratzel, N. Serpone, D.K. Sharma, J. Am. Chem. Soc. 107 (1985) 8054.
[19] N. Serpone, D. Lawless, R. Khairutdinov, E. Pelizzetti, J. Phys. Chem. 99 (1995) 16655.
[20] C. Arbour, D.K. Sharma, C.H. Langford, J. Phys. Chem. 94 (1990) 331.
[21] D.P. Colombo Jr., R.M. Bowman, J. Phys. Chem. 99 (1995) 11752.
[22] D.P. Colombo Jr., R.M. Bowman, J. Phys. Chem. 100 (1996) 18445.
[23] M. O'Neil, J. Marohn, G. McLendon, Chem. Phys. Lett. 168 (1990) 208.
[24] K. Stopper, J.K. Dohrmann, Z. Phys. Chem. 214 (2000) 555.
[25] W. Siripala, M. Tomkievicz, J. Electrochem. Soc. 129 (1982) 1240.
[26] F.F. Fan, A.J. Bard, J. Phys. Chem. 94 (1990) 3761.
[27] G. Redmond, D. Fitzmaurice, M. Graetzel, J. Phys. Chem. 97 (1993) 6951.
[28] G.K. Boschloo, A. Goossens, J. Phys. Chem. 100 (1996) 19489.
[29] G. Boschloo, D. Fitzmaurice, J. Phys. Chem. B 103 (1999) 2228.
[30] B. O'Regan, J. Moser, M. Anderson, M. Gratzel, J. Phys. Chem. 94 (1990) 8720.
[31] R.D. Cannon, K.G. Spears, Appl. Optics 34 (1995) 6834.
[32] J. Rudzki Small, L.J. Libertini, E.W. Small, Biophys. Chem. 42 (1992) 29.
[33] C.D. Borsarelli, S.E. Braslavsky, J. Phys. Chem. A 103 (1999) 1719.
[34] M.A. Rodriguez, S.E. Braslavsky, J. Phys. Chem. A 103 (1999) 6295.